(NASA-CR-200179) PARAMETERIZATION AND SCALING OF ARCTIC ICE CONDITIONS IN THE CONTEXT OF ICE-ATMOSPHERIC PROCESSES Final Report (Colorado Univ.) 13 p

N96-18731

Unclas

G3/46 0100343

Cooperative Institute for Research in Environmental Sciences

Division of Cryospheric and Polar Processes

University of Colorado at Boulder

Parameterization and Scaling of Arctic Ice Conditions in the Context of Ice-Atmospheric Processes

FINAL REPORT
NASA: NAGW-2598

R.G. Barry, K. Steffen, J.F. Heinrichs, J.R. Key,
J.A. Maslanik, M.C. Serreze and R.L. Weaver

Cooperative Institute for Research in Environmental Sciences
Division of Cryospheric and Polar Processes
University of Colorado
Boulder, Colorado 80309-0449

NOVEMBER 1995

University of Colorado

National Oceanic and Atmospheric Administration

Parameterization and Scaling of Arctic Ice Conditions in the Context of Ice-Atmospheric Processes

FINAL REPORT
NASA: NAGW-2598

R.G. Barry, K. Steffen, J.F. Heinrichs, J.R. Key,
J.A. Maslanik, M.C. Serreze and R.L. Weaver

Cooperative Institute for Research in Environmental Sciences
Division of Cryospheric and Polar Processes
University of Colorado
Boulder, Colorado 80309-0449

NOVEMBER 1995

1. INTRODUCTION

The sea ice cover affects the polar climate by regulating the exchange of heat, moisture, and momentum between the ocean and atmosphere. Energy exchanges are influence by seasonal changes in surface albedo and ice concentration. Area of surface divergence within the interior ice pack affect surface albedo, heat and moisture fluxes, ice mass balance, and ice morphology. Since these regions act as source regions for new ice growth and brine production, localized ice dynamics may substantially contribute to the salinity structure of the Arctic Ocean. An understanding of the ocean-atmosphere system in polar regions thus requires knowledge of the nature and variability of open water and thin ice areas within the ice cover under different atmospheric conditions. In particular, the short-term effects of leads and polynyas are poorly known.

2. OBJECTIVES

The goals of this project are to observe how the open water/thin ice fraction in a high-concentration ice pack responds to different short-period atmospheric forcings, and how this response is represented in different scales of observation. The objectives can be summarized as follows:

determine the feasibility and accuracy of ice concentration and ice typing by ERS-1 SAR backscatter data, and whether SAR data might be used to calibrate concentration estimates from optical and massive-microwave sensors;

investigate methods to integrate SAR data with other satellite data for turbulent heat flux parameterization at the ocean/atmosphere interface;

determine how the development and evolution of open water/thin ice areas within the interior ice pack vary under different atmospheric synoptic regimes;

compare how open-water/thin ice fractions estimated from large-area divergence measurements differ from fractions determined by summing localized openings in the pack;

relate these questions of scale and process to methods of observation, modeling, and averaging over time and space.

3. OVERALL APPROACH

The research focused on analysis of SAR and other data for (1) the Beaufort Sea-Canadian Basin sector of the central Arctic and (2) the Lady Ann Strait polynya adjoining the North Water of Baffin Bay where there are young ice types and strong temporal changes. An additional small case study was done combining remotely-sensed and field data for the Seasonal Sea Ice Monitoring and Modeling Site (SIMMS) in the Canadian Archipelago near Resolute (Barber et al. 1991). This report contains overall highlights of our findings and, in the Appendix, copies of the papers/reports deriving from this project that have been published to date.

4. DATA

The following data sets were used in these analyses:

4.1 Satellite Data

4.1.1 Beaufort Sea SAR Case Study

The data set used in our study of ice typing with Landsat and ERS-1 SAR (see Section 5.1) consisted of two overlapping pairs of Landsat TM and ERS-1 SAR images taken on April 15 and 18, 1992 covering a portion of the Beaufort Sea centered at 145° W, 73° N. The Landsat data was obtained from EOSAT Corporation and was geolocated, mapped to the UTM projection, and gridded to 25 m spatial resolution (slightly better than the actual 30 m resolution) in order to better match the SAR. Data from the C-band (5.3 GHz) SAR instrument aboard ERS-1 was obtained from the Alaska SAR Facility (ASF) at its full 12.5 m spatial resolution, resampled to 25 m resolution, and mapped to the Universal Transverse Mercator (UTM) projection. Coregistration of the image pairs was a challenging process was accomplished by the use of successively smaller offsets determined visually and the use of color composite images for precise registration.

4.1.2 North Water SAR Time Series

For our study of the Lady Ann Strait polynya (see Section 5.2), we obtained from ASF a series of 30 images of the Lady Ann Strait region covering a period of 5 months between Nov. 20, 1991 and April 17, 1992. The images were of the low resolution product, with 100 m resolution, and each measured 100 km on a side. The images were calibrated using the standard GPS technique, converted to decibels (dB), and scaled.

4.1.3 Beaufort Sea SAR Time Series

The data used in our study of ice model validation with forward simulation of SAR data (see Section 5.3 and 5.4) and responses to synoptic systems covered a region in the Beaufort Sea centered at 78° N, 153° W during a 13-month period from October 1991 to November 1992. A series of 31 images from the ERS-1 C-band SAR was obtained from the Alaska SAR Facility (ASF) and calibrated using the operational ASF algorithm. As part of the calibration process, the data were scaled from Digital Number (DN) values to backscatter values in dB.

4.2 Meteorological Data

We obtained concurrent meteorological data from the National Meteorological Center (NMC), including surface air temperature, and pressure. Geostrophic wind velocity and direction fields were derived from the NMC pressure data.

Gridded NMC mean sea-level pressure data for 1952-1992 were utilized to develop a classification of daily synoptic pressure-pattern types and a data base of the daily position and central pressures of synoptic-scale cyclones and anticyclones in the Arctic. The NMC winds were also used to drive the 2-D ice models.

4.3 Model Output

Model fields of daily winds, ice motion, ice motion area thickness, growth, and divergence generated by the Polar Ice Prediction System (PIPS) at Naval Ocean Atmospheric Research Laboratory (NOARL) were acquired through an agreement with Ruth Preller. Ice motion and ice

concentration data were also obtained from a basic Hibler-type model as well as a 2-D model revised to include specific ice layers (first-year, second-year, and multiyear ice), more detailed turbulent flux processes, a finer grid mesh, and finer time steps. Specific model runs were performed to coincide with the time series of SAR data acquired for the Beaufort Sea. Specific outputs saved from these runs include ice type area and thickness, open water fraction, and energy fluxes.

4.4 Buoy Data

Buoy products (buoy motion, motion derivatives, and buoy temperatures) were acquired from the Arctic Ocean Buoy Program (AOBP). These data were used in conjunction with ice model output and NMC winds to depict large-scale and finer-scale ice motion fields and to calculate divergence and shear terms for ice-production estimates.

4.5 Field Data

Field data available from the SIMMS camp near Resolute, NWT (Barber et al., 1991) included surface albedo, meltpond conditions, ice type, snow conditions, and full suite of meteorological and energy balance data.

5. STUDIES OF ICE CHARACTERISTICS

5.1 Intercomparison of ERS-1 SAR and Landsat for ice classification

Our study of ice typing, which has been described in Steffen and Heinrichs (1994, included in the Appendix), had two major objectives. The first was to evaluate SAR-based ice typing in general using Landsat TM data, and the second and more specific was to assess the performance of the operational classifier used in the Geophysical Processing System (GPS) at the Alaska SAR Facility (ASF). The data set used in our work consisted of two overlapping pairs of Landsat TM and ERS-1 SAR images covering a portion of the Beaufort Sea. Once coregistration and subsetting of the image pairs were complete, images of TM band 4 (760-900 nm) and TM band 6 (10.4 - 12.5 micro-m in the thermal infrared) were used to select training data regions for each of seven ice types as defined by the standard WMO nomenclature. The training data were used to define a supervised classification based on Landsat TM band 4. Figure 1 shows a graphical representation of the results of our statistical analysis of the SAR pixels assigned to each ice type as defined by the Landsat supervised classification. The TM data shows a distinct separation between most ice classes with, however, some overlap between first year ice (FYI) and old ice (OI). This is due to the snow cover over both ice types causing their albedos to be very similar. The SAR data, however, shows major overlaps between many ice types. OI and FYI can be readily distinguished in the SAR data, but the nilas (NI), grey ice, and grey-white ice categories have substantial overlap, both with each other and with the OI and FYI classes. The ice free (IF) areas also have backscatter values similar to the solid ice types, but different for the two days studied. This is a consequence of wind roughening (increased backscatter caused by wind-formed capillary waves on the ocean surface).

Our evaluation of the GPS classifier was based on the results of the SAR/Landsat comparison described above. The GPS ice types are somewhat different from the WMO list, and the training data was recombined to reflect this difference. While the two classifications agree well for FYI-1 and OI, significant differences in the means exist for the combined IF/NI/YI and the FYI-2 classes. The GPS threshold used for IF generally restricts identification to calm wind

conditions. IF areas identified in the TM imagery, because of the moderate winds on April 16, have higher backscatter values and are misclassified by the GPS as other types. By calculating the percentage of correct decisions made by the GPS classifier as compared to the TM-derived classification, we were able to quantitatively assess the GPS performance. OI classification accuracy is the best of the four GPS types with FYI-1 a distant second. IF/NI/YI and FYI-2 categories do not perform well, most likely due to misclassification of IF pixels.

The final portion of the study involved an examination of the effectiveness of using the SAR and TM data together in a multispectral classification. SAR is superior for separating FYI and OI, where Landsat has advantages for IF, NI, and YI, and the combination of both offers possibilities for performing operational ice typing. We evaluated the performance of several channel combinations against the training data used in the original SAR/Landsat classification. The combination of SAR and single TM visible channels (channels 2,3, or 4) was found to improve accuracy over TM for all but the FYI types. Adding multiple visible channels improved accuracy for FYI-2, and adding channel 6 (thermal infrared) resulted in an accuracy greater than or equal to 90% for all types. We concluded that combining SAR and electro-optical data would clearly provide superior ice classification products, and that further research in this area would be useful.

5.1.1 SIMMS Case Study

In addition to the combination of JERS-1 L-band and ERS-1 C-band imagery to investigate improvements in ice feature identification, JERS-1 SAR and aircraft SAR were combined with JERS-1 optical-band imagery to study surface melt features. Field observations of meltpond coverage on a multiyear ice floe near Resolute Bay were used to determine the correspondence between low backscatter areas in SAR vs. reduced-albedo conditions during melt. Different melt conditions over the multiyear floe compared to adjacent first-year ice were readily apparent. The combination of a SAR time series with optical-band data suggest possibilities for mixed-pixel algorithms to estimate meltpond coverage (Maslanik and Heinrichs, 1995).

5.2 Surface Process Study of the Lady Ann Strait Polynya

It is becoming more widely realized that coastal polynyas have a major influence on the heat and energy balance of the ice-covered seas. Furthermore, the large rates of ice formation and brine production typical of polynyas are important climatic factors. Our objective in this study (Steffen and Heinrichs, 1993) was to examine ice cover variations and the underlying physical processes in one polynya, making use of the rapid repeat coverage during the ERS-1 ice cycle and the SAR instrument's high resolution and ability to penetrate clouds and darkness.

The ice cover in the Lady Ann Strait, northwestern Baffin Bay, has been studied extensively in the past using visible and passive microwave low-resolution satellite imagery. This area is known to have a persistent thin ice cover throughout winter, whereas the surrounding pack ice areas consist mainly of thick first-year ice. A total of 30 different ERS-1 SAR scenes from the Lady Ann Strait polynya were acquired for the time period of winter 1991-92 and 1992-93. The dynamic change of the Lady Ann Strait polynya ice cover has been studied throughout winter based on low-resolution (100 m) and high-resolution (12.5 m) SAR imagery. Analysis of the time-series analysis shows that young and thin ice are constantly advected from the Lady Ann Strait towards Devon Island and northwestern Baffin Bay. The 3-day repeat cycle of the ERS-1 satellite enables the study of the growth rates of various ice types within the polynya. This time sequence provides a valuable data set that documents the change in the backscatter coefficient of

open water, young ice and thin ice with time. Dramatic changes in the backscatter coefficient for young ice types during rapid growth have been observed. This information is valuable for the derivation of ice thickness, and consequently for the estimation of turbulent and radiative surface energy fluxes at the ocean-atmosphere interface of a polynya. Sea ice backscattering time series over a three month period were studied for multi-year ice, first-year ice rough, and first-year ice smooth with a temporal resolution of three days.

The time series (Figure 2) show that multi-year ice has a stable backscatter coefficient, whereas, the first-year ice with a rough surface shows a decrease of the backscattering coefficient with time. Further, the changes in first-year backscattering coefficients seem to be correlated with meteorological conditions, such as temperature and vapor flux.

5.3 Studies of the Seasonal Cycle of Sea Ice Using SAR Data

One of the major tools for studying the response of sea ice to radiative, wind, and thermal forcing is the use of models of ice dynamics and thermodynamics. We developed a technique of validating such models by forward simulation, or the generation of estimated backscatter values directly from the physical model output. This approach eliminates common validation problems with geophysical parameters obtained from statistical algorithms by taking advantage of the reduction of ambiguity between physical state and backscatter inherent in the statistical algorithms. A simple model of sea ice backscatter, based on area-weighted sums of the backscatter contribution of various ice types and the variation of open water backscatter with wind speed, was coupled to the physical model and used to estimate the C-band backscatter over a one year period at a site in the Beaufort Sea. A comparison with actual ERS-1 SAR data for the same time period revealed good agreement during the late autumn, spring, and fall periods and large differences during the melt and freeze up periods in summer and early autumn. After we included parameterizations of the backscatter effects of wet snow, meltponds, and frost flowers on young ice, the performance of the combined physical/backscatter model during melt and freeze up improved dramatically. This study, which has been described in a recently submitted paper (Heinrichs et al. 1995, included in the Appendix) not only demonstrated the utility of the forward simulation approach for validating physical models with SAR data, but showed that forward simulation can be used to identify important processes that need to be included in the physical models.

5.4. Ice Response to Atmospheric Synoptic Conditions

Scale dependencies exist in the response of the ice pack to atmospheric synoptic conditions. For example, localized opening and closing or shear may not be reflected in large-scale diverence calculations, and the changes in ice cover at a given location are influenced by conditions elsewhere in the ice pack. In turn, remotely-sensed data may yield different estimates of ice motion or open water production depending on the sensor type and spatial resolution. To investigate these issues, we intercompared time series of SAR imagery, SSM/I data, AVHRR imagery, and ice model output. Since each of these time series addresses different space and time scales, the intercomparison sheds light on how processes differ across scales, and how the representations of these processes are affected by observation method.

Two manuscripts have been prepared that summarize these results. The first manuscript focuses in particular on ice motion and divergence/shear estimates (Fowler et al., 1995). The second considers the time series of open water production and ice type as depicted in the

different data sets (Maslanik et al., 1995). Since neither paper is yet in print, the results are summarized below.

Variations in ice motion and open-water production associated with synoptic systems are depicted in different image types and in dynamic-thermodynamic model simulations using viscous-plastic and cavitating fluid ice rheologies. Fowler et al., (1995) find good agreement between observed and simulated ice velocities, within the central-pack region studied, with rapid shifts in ice drift speed and direction in response to the weather systems. The AVHRR and SAR-derived motion fields show considerable local variability but are consistent with the general drift pattern simulated using geostrophic winds. Simulations show slightly greater divergence-related reductions in concentration than is seen in SAR data, but less change in concentration and first-year ice fraction than is inferred from SSM/I imagery. The cavitating fluid model produces higher drift speeds during rapid drift, resulting in greater open-water production of 1-2% relative to the viscous-plastic rheology. Significant correlations are found between changes in SSM/I-derived concentrations and simulated divergence and shear over about 40% of the study area, with a variety of other possible factors including errors in the microwave retrievals and insufficient physics in the model contributing to the lack of correlation over the remaining area.

Changes within the consolidated ice pack are examined in detail Maslanik et al, (1995) for October 1991. The analysis is then extended to consider general conditions from October 1991 through June 1992. The SAR, SSM/I, and modeled concentrations concur generally in showing a 1-5% decrease in ice fraction during the passage of low-pressure systems through the study area. AVHRR imagery indicate a greater proportion of thin ice within the pack, but comparable decreases in concentration. While changes in SSM/I-derived open-water fractions are similar to changes in the other data sets, the SSM/I data suggest substantial increases in first-year ice concentration indicative of the formation and re-freezing of open water areas. Sensible heat fluxes calculated using open-water and ice-type fractions from the SAR and SSM/I imagery point out the sensitivity of heat transfer estimates to the data types and classification method used to derive ice information.

5.5 Lead statistics/scale and satellite resolution

The impact of sea ice leads on regional scale climate is difficult to assess without more information on their distribution in both space and time. Satellite data provide the spatial and temporal coverage needed for climate studies, but most sensors cannot adequately resolve small surface features such as leads. If we need lead width, spacing, and orientation distributions to estimate turbulent fluxes over sea ice, we need to understand the relationship between sensor resolution and lead characteristics.

While there have been studies of the effect of sensor resolution on parameter retrieval, the approaches have been empirical and no concise statement of the relationship between fractional coverage and sensor resolution has been given. A complete analytical description of the problem is difficult at best, involving geometrical (viewing geometry), spectral (band location and width), radiometric (signal-to-noise ratio, quantization levels), and spatial (sensor resolution or pixel size) properties. A first attempt at an analytical approach to the problem was made by Key (1994). The effect of sensor field-of-view on the estimate of lead area fraction was examined by modelling the unknown distribution of subpixel area fraction with the beta distribution, whose two parameters depend on the true fractional area coverage, the pixel size, and the spatial structure of the geophysical field expressed in the exponential autocovariance function. It was

shown that the rate and direction of change in total area fraction with changing pixel size depends on the true area fraction, the spatial structure, and the thresholding operation used. The complete statistical-analytical model is described in Key (1994).

Since a complete analytical model of the effect of sensor FOV on parameter estimation is not currently available, we also examined this problem empirically. Remote sensing of leads using satellite data, specifically AVHRR thermal and Landsat visible-band imagery, was examined with respect to lead width, orientation, and area fraction estimates. The geometrical aspects of the sensor were simulated so that the effect of sensor field-of-view on retrieved lead width statistics could be assessed. This was done using Landsat data and simulated lead networks degraded to AVHRR pixel sizes. The analyses illustrate how leads of sufficiently high contrast tend to "grow" with increasing pixel size and how small or low contrast leads disappear. The relationship between lead contrast and the width/field-of-view ratio was also examined in order to determine the limits of lead detectability, and illustrated the multi-valued nature of the problem of lead width retrieval. To help quantify the importance of changes in lead statistics, turbulent heat flux was calculated as a function of lead width and lead fraction. It was shown that pixel size has a substantial effect on estimates of turbulent heat transfer from leads to the atmosphere. Details are given in Key et al. (1994).

5.6 Effects of leads on turbulent heat-flux

One of the features of SAR data is the ability to discriminate leads from surrounding pack ice. However, as noted in Section 5.1 existing spaceborne SAR systems provide only crude and inaccurate information on the thickness of ice in refrozen leads, and in some cases cannot distinguish whether leads are open or refrozen. With this in mind, SAR data can provide useful information on lead area and morphology, but relatively poor information on thermodynamic conditions within leads. Thus, objectives for this task were to investigate: 1) the importance in ice models of lead width and lead count information compared to the importance of lead-ice thickness information; and 2) how a sea ice model might best take advantage of the lead morphology information.

Experiments were conducted with lead width and ice thickness information to determine their effects, via fetch and stability, on turbulent flux estimates. A fetch and stability dependent model of bulk transfer coefficients was combined with a 1-D energy balance model and boundary layer model to assess these effects and to test scaling parameterizations (Maslanik and Key, 1995). Fluxes over leads were found to be quite sensitive to fetch for small changes in fetch (10 m to 200 m), but this sensitivity was reduced as ice thickness increased within a lead (e.g., between open and refrozen leads). Parameterizing fetch across sampling scales was also addressed. Fluxes integrated over a lead-width distribution differed considerably from fluxes estimated using a lead-width mean. However, this mean could be used to construct a statistical width distribution to improve flux estimates.

Our 2-D model was revised to include a parameterization of the fetch and stability dependency discussed in Maslanik and Key (1995). In the 2-D simulations, total ice production in the Arctic increased substantially as the proportion of small leads was increased relative to the total open water area. This response is due to the higher heat-loss rate from smaller leads. In this ice-only simulation, the excess heat was not allowed to warm the overlying atmosphere. Coupled ice-atmosphere modeling is therefore needed to quantify the strength and sign of this lead morphology-heat loss feedback. However, the 1-D and 2-D simulations suggest that while GCMs are being improved to include lead fraction, the methods used to parameterize fluxes from these leads could have a significant effect on the simulations.

6. CONCLUSIONS

The objectives identified in the original proposal have all been addressed and considerable progress has been made toward the overall goal of improving our understanding of the responses of open water/thin ice areas in high-concentration ice fields to atmospheric forcings and how such responses are characterized at different observational scales. Diverse satellite data (ERS-1, JERS-1, AVHRR, Landsat), field observations, buoy data and meteorological data were used in the analyses.

Highlights of the project's accomplishments are:

- Development and assessment of a SAR-based ice type classification using Landsat data. SAR gives good results sin separating FYI and old ice whereas Landsat is superior for ice-free areas, nilas and young ice categories. Clearly, a combined approach is essential. Summer meltpond coverage can possibly be estimated via mixed pixel algorithms by combining SAR and optical band data.

- The annual cycle of ice in the Beaufort Sea has been analysed using SAR backscatter data. A forward simulation approach was successful in identifying key processes in physical models and in validating such models. Parameterizations for wet snow, meltponds and frost flowers on young ice dramatically improved the performance of a combined physical/backscatter model during freeze up and melt.

- Rapid changes in ice conditions during freeze-up are strongly determined by divergence forced by low pressure systems. In relation to this, a cyclone climatology for the Arctic was prepared for 1952-92.

- Ice dynamics and related physical processes in the Lady Ann Strait polynya during two winters were documented in detail using SAR data. Young and thin ice is continually produced and advected towards Devon Island and northwestern Baffin Bay. The data can also be used to derive estimates of surface energy fluxes to the atmosphere.

- Ice motion can be optimally determined over large areas using a combination of SAR and AVHRR data, in conjunction with buoy velocities. Good agreement is obtained in comparisons between these observations and simulations of ice motion with current sea ice models.

- The sensor resolution is a critical factor in obtaining lead statistics. The problem is complex, involving viewing geometric, radiometric, spectral and spatial characteristics. A statistical-analytical model for determining true lead area fraction has been developed.

- The importance of pixel size in estimating turbulent heat fluxes from leads has also been quantified. These fluxes shown to be sensitive to atmospheric fetch and stability, but the sensitivity decreases in refreezing leads. Coupled ice-atmosphere models need to design appropriate parameterizations for fluxes from leads in sea ice.

- Preparation of a doctoral thesis, by J. Heinrichs, supported by the project is in progress.

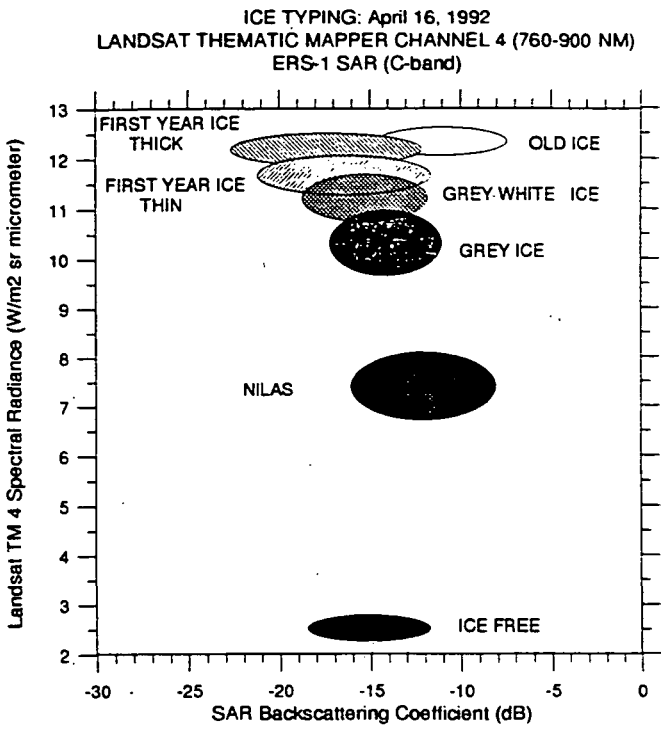

Figure 1. Graphical representation of ice type statistics as determined from SAR ERS-1 data and a supervised classification of Landsat TM data.

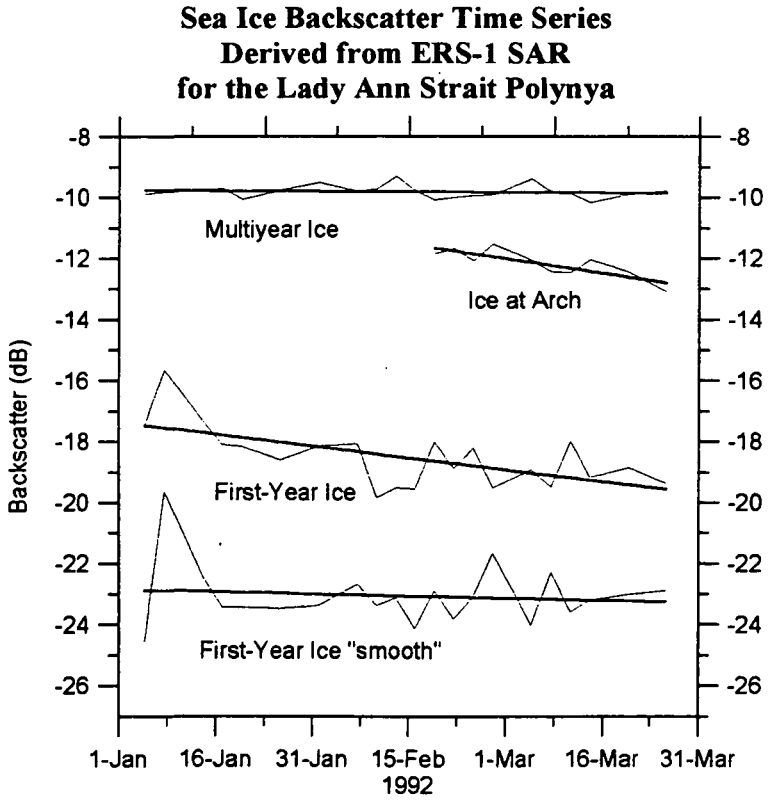

Figure 2. Time series of backscatter for FY1 and MY1 in Lady Ann Strait Polynya.

7. REFERENCES CITED

Barber, D.G. et al., 1991. Measuring climatic state variables from SAR images of sea ice: The SIMMS SAR validation site in Lancaster Sound. *Arctic* 44 Suppl 1:108-21.

Fowler, C., J.A. Maslanik, W.J. Emery, 1995. Observed and simulated responses of a high-concentration ice cover to synoptic weather systems (in preparation).

Heinrichs, J., J. Maslanik, and K. Steffen, The seasonal cycle of sea ice in the Beaufort Sea: A comparison of model output and ERS-1 SAR data using a forward simulation approach, *J. Geophys. Res.*, submitted November 1995.

Key, J.R. 1994. The area coverage of geophysical fields as a function of sensosr field-of-view. *Remote Sens. Environ.* 48:339-346.

Key, J., J.A. Maslanik, and E. Ellefsen, 1994. The effects of sensor field-of-view on the geometrical characteristics of sea ice leads and implications for large-area heat flux estimates. *Remote Sensing Environ.*, 48:347-357.

Kwok, R. and G. Cunningham, 1992: Geophysical Processor System data user's handbook, NASA, JPL, Pasadena, CA, JPL D-9526 (draft).

Maslanik, J.A., C. Fowler, J. Heinrichs, R.G. Barry, and W.J. Emery, 1995. Remotely-sensed and simulated variability of Arctic sea-ice concentrations in response to atmospheric synoptic systems. Int. J. Remote Sensing, (in press).

Maslanik, J.A. and J. Key, 1995. On treatments of fetch and stability sensitivity in large-area estimates of sensible heat flux over sea ice. *J. Geophys. Res.*, 100, C3, 4573-4584.

Maslanik, J.A. and J. Heinrichs, 1995. Sea-ice feature mapping using JERS-1 imagery. In: *Final Report JERS-1/ERS-1 System Verification Program, V. II,* MITI/NASDA, Japan. pp.501-517.

Steffen, K. And Heinrichs, J. 1994. Feasibility of sea ice typing with synthetic aperture radar (SAR): Merging of Landsat thematic mapper and ERS-1 SAR satellite imagery. *J. Geophys. Res.*, 99(C11): 22,413-22,424.

Steffen, K., and J. Heinrichs, 1993. Surface Process Study of the Lady Ann Strait Polynya with ERS-1 SAR Imagery, *Space at the Service of our Environment ESA SP 361* p.107.

8. PUBLICATIONS DERIVED

Carsey, F.D., R.G. Barry and W.F. Weeks, 1992. Introduction Ch. 1. In: *Microwave remote sensing of sea ice,* (ed.) F.D. Carsey AGU Monograph 68:1-7.

Carsey, F.D., R.G. Barry, D. Rothrock and W.F. Weeks, 1992. Status and future directions of remote sensing of sea ice, Ch. 26. *Microwave remote sensing of sea ice,* (ed.) F.D. Carsey AGU Monograph 68:443-446.

Fowler, C., J.A. Maslanik, W.J. Emery, 1995. Observed and simulated responses of a high-concentration ice cover to synoptic weather systems (in preparation).

Heinrichs, J., J. Maslanik, and K. Steffen, The seasonal cycle of sea ice in the Beaufort Sea: A comparison of model output and ERS-1 SAR data using a forward simulation approach, *J. Geophys. Res.*, submitted November 1995.

Key, J. 1994. The area coverage of geophysical fields as a function of sensor field-of-view. *Remote Sensing Environ.*, 48:339-346.

Key, J., J.A. Maslanik, and E. Ellefsen, 1994. The effects of sensor field-of-view on the geometrical characteristics of sea ice leads and implications for large-area heat flux estimates. *Remote Sensing Environ.*, 48:347-357.

Maslanik, J.A. and J. Key, 1995. On treatments of fetch and stability sensitivity in large-area estimates of sensible heat flux over sea ice. *J. Geophys. Res.*, 100, C3, 4573-4584.

Maslanik, J., Fowler, C., Emery, W.J., Heinrichs, J. And Barry, R.G. 1994. Ice-atmosphere interactions in the central Arctic Remotely-sensed and simulated ice concentration and motion. *Proceedings Second ERS-1 Symposium. Space at the Service of our Environment. ESA-sp-361.* European Space Agency, Paris. Pp.373-378.

Maslanik, J.A. and J. Heinrichs, 1995. Sea-ice feature mapping using JERS-1 imagery. In: *Final Report JERS-1/ERS-1 System Verification Program, V. II,* MITI/NASDA, Japan. pp.501-517.

Maslanik, J.A., C. Fowler, J. Heinrichs, R.G. Barry, and W.J. Emery, 1995. Remotely-sensed and simulated variability of Arctic sea-ice concentrations in response to atmospheric synoptic systems. *Int. J. Remote Sensing,* (in press).

Serreze, M.C., J.E. Box, R.G. Barry, J.E. 1993. Walsh, Characteristics of Arctic synoptic activity, 1952-1989, *Meteorol. Atmos. Phys.* 51:147-164.

Steffen, K. And Heinrichs, J. 1994. Feasibility of sea ice typing with synthetic aperture radar (SAR): Merging of Landsat thematic mapper and ERS-1 SAR satellite imagery. *J. Geophys. Res.*, 99(C11): 22,413-22,424.

Steffen, K., J. Heinrichs, J. Maslanik, and J. Key, 1993. Sea ice feature and type identification in merged ERS-1 SAR and Landsat Thematic Mapper Imagery, *Space at the Service of Our Environment. Proceedings of the First ERS-1 Symposium,* Cannes, France, 1992, p.361,v.1 European Space Agency, Paris.

Steffen, K., and J. Heinrichs, 1993. Surface Process Study of the Lady Ann Strait Polynya with ERS-1 SAR Imagery, *Space at the Service of our Environment. Proceedings of the First ERS-1 Symposium.* Cannes, France, 1992. Abstracts, p. 107.